

# Multi-walled carbon nanotubes functionalized with a ultrahigh fraction of carboxyl and hydroxyl groups by ultrasound-assisted oxidation

Shaolei Liang<sup>2</sup> · Guangfen Li<sup>1,2</sup> · Run Tian<sup>2</sup>

Received: 22 September 2015 / Accepted: 12 December 2015 / Published online: 21 December 2015  
© Springer Science+Business Media New York 2015

**Abstract** In this study, multifunctionalized multi-walled carbon nanotubes (MWCNTs) were functionalized through a novel three-step oxidation approach assisted by ultrasonication. We chose an oxidation system with three oxidation agents, concentrated sulfuric acid, potassium permanganate, and hydrogen peroxide. In comparison to non-ultrasonic processes, the effect of our ultrasound-assisted process on the carboxyl and hydroxyl content of the modified MWCNTs (m-MWCNTs-2) was discussed using Fourier transform infrared spectroscopy and X-ray photoelectron spectroscopy. The results verified that the ultrasound-assisted oxidation process is much more effective than those without ultrasonication; a higher hydroxyl content of 11.88 at.% and a carboxyl content of 8.82 at.% in the m-MWCNTs-2 were estimated. A Raman spectrum showed an increased value of  $I_D/I_G$ , which proved the presence of defect sites or the functional groups on the surface of the MWCNTs. Thermogravimetric analysis was found to semiquantitatively evaluate the amount of carboxyl and hydroxyl groups in the MWCNTs. A better dispersion of the m-MWCNTs-2 in ethanol or water was expected from a photograph, a particle size analysis, and field emission scanning electron microscopy. High-resolution transmission electron microscopy revealed that the diameter of the m-MWCNTs-2 was reduced to a lesser

degree using the ultrasonication assistance than of those generated without ultrasonication.

## Introduction

Carbon nanotubes (CNTs) have found many applications in areas, such as tissue engineering [1], gas separation membrane [2], and polymer composites [3], due to their extraordinary thermal [4], mechanical [5], and electrical properties [6]. However, the applications of CNTs in different fields have been limited by the strong intrinsic van der Waals force between the CNTs, which results in self-aggregation and the formation of the bundles or agglomerates of the nanotubes in liquid media or in a polymer matrix. To efficiently maintain and transfer their unique properties into different materials and to actualize the potential applications using CNTs, many efforts have been focused on improving the dispersion of CNTs in solvents and the interfacial interaction of CNTs with other compounds [7]. To achieve this purpose, several processes, including mechanical dispersion (ultrasonication, ball milling, extrusion etc.) [8] and surface modifications of CNTs [9], were explored.

Chemical modification processes with different oxidizing acids or oxidants are most prevalent due to their efficiency in decorating the CNT surface with the desired functional groups and altering the surface composition. The introduction of functional groups, either hydroxyl (–OH) or carboxyl (–COOH) groups, into CNTs can improve not only the CNT dispersibility in various solvents but also the interaction with other compounds, such as polymers [10]. The chemical oxidation of CNTs with different oxidizing agents, such as  $H_2SO_4$ ,  $HNO_3$ ,  $H_2O_2$ ,  $O_3$ , and potassium permanganate ( $KMnO_4$ ), has been reported [11]. The

✉ Guangfen Li  
liguangfen@tjpu.edu.cn

<sup>1</sup> State Key Laboratory of Separation Membranes and Membrane Processes, Tianjin Polytechnic University, Tianjin 300387, China

<sup>2</sup> School of Materials Science and Engineering, Tianjin Polytechnic University, Tianjin 300387, China

application of  $\text{H}_2\text{SO}_4$ ,  $\text{HNO}_3$  and  $\text{KMnO}_4$  can introduce carboxyl groups into nanotubes, whereas mild oxidants, such as  $\text{H}_2\text{O}_2$  and  $\text{O}_3$ , tend to generate hydroxyl groups. A combination of two oxidizing agents may result in two functional groups presenting simultaneously on the CNTs. Multifunctional CNTs commonly contain two or three different functional groups, thus possessing higher chemical reactivity and selectivity, which are considered to be a major advantage over other functionalized CNTs [9]. Alternative methods for the oxidation of graphene provide another possibility to realize oxidation of CNTs. Multi-walled nanotubes and graphene are composed of  $\text{sp}^2$ -hybridized carbons, and both can be easily oxidized at the defects at the ends. The most commonly used oxidation process for graphene is the Hummers' method, and the corresponding mechanisms of this method have been discussed in the literature [12]. In fact, different modified Hummers method has been also widely applied for unzipping CNTs with well-established oxidation mechanisms [13].

Mechanical mixing can improve the dispersion of CNTs in solvents, but some damage to the CNTs and reductions in their length can hardly be avoided. UV treatment [14], plasma treatment [15], and microwave irradiation [16] have been utilized either for incorporation of surface oxygen or for the attachment of diverse functional groups to the CNTs. During the oxidation process, mechanical mixing, such as the conventional reflux method, was generally utilized. Compared with the reflux method, the use of ultrasonication [17] for the functionalization of CNTs may lead to a higher content of carboxyl, carbonyl, and hydroxyl groups on the MWCNT surfaces because the sonication process may create more surface area and defect sites for the attachment of functional groups. Saleh et al. [18] have successfully debundled carbon nanotubes with ultrasonication probe, and the debundled carbon nanotubes were shortened, and the structure integrity of the tubes was destroyed. Hennrich et al. [19] proposed the mechanism of cavitation-induced scission of single-walled carbon nanotubes. A mild acid oxidation with ultrasound (100 w, 42 kHz) reported by Avilés et al. [20] was found to well purify the tubes. With acoustic cavitations, a high content of hydroxyl groups on the multifunctional MWCNTs was obtained using an  $\text{H}_2\text{O}_2$  solution as the oxidation system [8]. The irradiation of liquid from ultrasound waves leads to the growth and collapse of micro bubbles to produce local high temperatures and pressures. This energy promotes the dispersibility of the MWCNTs, creating larger surface areas and more defect sites for a rapid reaction [21]. To the best of our knowledge, the multifunctionalization of the MWCNTs with a higher content of carboxyl and hydroxyl groups has rarely been reported.

To obtain multifunctional MWCNTs with a higher content of carboxyl and hydroxyl groups within a short reaction time, the oxidation system was designed based on the Hummers' oxidation system assisted by ultrasonication. In this study, a novel and simple multifunctionalized approach for modifying the MWCNT surfaces with both carboxyl and hydroxyl groups was performed with an ultrasound-assisted three-component oxidant ( $\text{H}_2\text{SO}_4$ ,  $\text{KMnO}_4$ ,  $\text{H}_2\text{O}_2$ ) system. The effects of ultrasound in the oxidation process on the content of the carboxyl and hydroxyl groups and the dispersibility of the MWCNTs in solvents were discussed in comparison with commercial pristine MWCNTs and MWCNTs-COOH. Changes in the surface chemical structure and in the content of functional groups were evaluated using a combination of Fourier transform infrared (FTIR) spectroscopy, Raman spectroscopy, X-ray photoelectron spectroscopy (XPS), and thermogravimetric analysis (TGA). The dispersity of different MWCNTs in either ethanol or water was analyzed by photography and a particle size analyzer. In addition, the surface morphology of four MWCNTs was imaged by field emission scanning electron microscopy (FESEM) and high-resolution transmission electron microscopy (HR-TEM) to confirm the improved dispersibility and to identify the damages on the surface of the nanotubes resulting from the oxidation process.

## Experimental

### Materials and solvents

Two different commercially available pristine multi-walled nanotubes (p-MWCNTs, length 10–30  $\mu\text{m}$ ), and carboxylated multi-walled nanotubes (p-MWCNTs-COOH, length 10–30  $\mu\text{m}$ , carboxyl content 3.86 wt%) with purities higher than 95 % were supplied by Chengdu Organic Chemistry Research Institute. Concentrated sulfuric acid ( $\text{H}_2\text{SO}_4$ ), hydrochloride acid (HCl), sodium nitrate ( $\text{NaNO}_3$ ), potassium permanganate ( $\text{KMnO}_4$ ), hydrogen peroxide ( $\text{H}_2\text{O}_2$ ), and ethanol were analytical grade and were obtained from Chengdu Kelong Chemical Co., Ltd. and Tianjin Fengchuan Chemical Co., Ltd.

### Procedure

A three-component oxidant system, including concentrated sulfuric acid, hydrogen peroxide, and potassium permanganate, was applied to functionalize the MWCNTs through an ultrasound-assisted oxidation procedure with the power of 150 W and the frequency of 40 kHz. Because the temperature varies with the addition of different oxidants from 11, 35–45, to 60 °C, a three-stage oxidation procedure as

stage I, stage II, and stage III was performed as follows: Stage I: p-MWCNTs (0.1 g) were mixed with  $\text{NaNO}_3$  (0.1 g) and  $\text{H}_2\text{SO}_4$  (60 ml 78 wt%). Then, the mixture was stirred and ultrasonicated for 40 min at 11 °C in an ice bath. This process was performed to minimize the damage to the MWCNT sidewalls, limit the reaction speed during the formation of active sites on the nanotubes, and provide potential active sites for attaching functional groups in the next stage. Stage II:  $\text{KMnO}_4$  (0.2 g) was slowly added into the mixture and ultrasonicated for 2 h at 35–45 °C. The same procedure was performed without using ultrasonic treatment for a comparison. A mild temperature was used to minimize the damage to the MWCNTs as they are exposed to the strong oxidant, concentrated  $\text{H}_2\text{SO}_4$ . However, the ultrasound used in this study served to improve the dispersibility of CNTs, increasing the number of active defect sites and accelerating the reaction rates. Multi-groups, such as carboxyl, hydroxyl, and carbonyl groups, were supposed to attach to the MWCNT sidewalls. Stage III: An  $\text{H}_2\text{O}_2$  solution (20 ml, 30 wt%) was slowly added into the mixture, and the CNTs were further chemically functionalized with  $\text{H}_2\text{O}_2$  under reflux at 60 °C for 40 min.

This oxidation process was expected to further increase the content of hydroxyl groups attached to the MWCNTs. The synthetic route of the multifunctionalization of the MWCNTs is illustrated in Fig. 1.

When the mixture was cooled to room temperature, it was first washed three times with a diluted HCl solution (5 wt%) and then centrifuged under a speed of 8000 r/min to remove the residue from the reagents. Afterward, the mixture was rinsed several times by deionized water until

the pH of the mixture was neutral. The centrifuged MWCNTs solution was poured into an aluminum foil container and dried at 70 °C overnight under vacuum. The dried product dispersed in ethanol was ground for 10 min in an agate mortar and then dried again. The functionalized MWCNTs in stage I and the functionalized MWCNTs without or with ultrasonication in stage III were abbreviated m-MWCNTs, m-MWCNTs-1, and m-MWCNTs-2.

## Characterization

A series of characterizations were performed to verify the changes to the chemical composition, the content of functional groups, the dispersibility, and the surface morphology of different MWCNTs. To identify the functional groups attached to the MWCNTs, FTIR spectra of five different MWCNTs were recorded with a KBr pellet on a spectrometer (TENSOR37, Bruker, Germany) ranging from 500 to 4000  $\text{cm}^{-1}$ . Raman spectra were obtained in a Raman spectrophotometer (DXR, Thermo Fisher Scientific, U.S.) with the 532 nm line of an Ar-ion laser. To further identify the varieties and content of the functional groups grafted onto the MWCNTs, X-ray photoelectron spectroscopy (XPS, K-Alpha, Thermo Fisher Scientific, U.S.) was utilized. A digital camera was used to record the correlation of the dispersibility of the MWCNTs in ethanol with time. Furthermore, the particle size distribution of the MWCNTs in water was analyzed by a laser particle size analyzer (BT-9300H, Dandong Better size Instruments Ltd., China). The samples were obtained by dispersing the nanotubes in deionized water and ultrasonating for

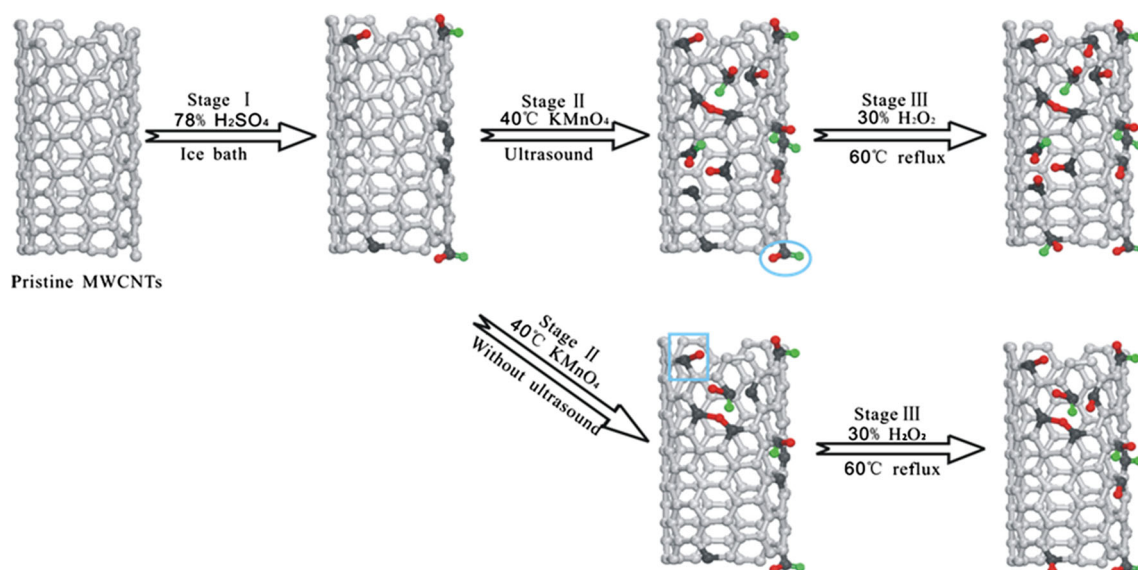


**Fig. 1** Synthetic route for the multifunctionalization of MWCNTs with carboxyl and hydroxyl groups, which are marked by an elliptical region and rectangular region, respectively. Atoms in black, red, and

green represent the active sites of carbon atoms, C–O groups, and C=O groups, while the hydrogen atoms are not displayed (Color figure online)

10 min. The surface morphologies and quality of sidewalls of the four different MWCNTs were studied through field emission scanning electron microscopy (FESEM, Hitachi-4800, Hitachi Limited, Japan) and high-resolution transmission electron microscopy (HR-TEM, JEM-2100, JEOL, Japan), respectively. The samples for FESEM were prepared by dispersing MWCNTs in ethanol and ultrasonating for 10 min. Subsequently, a few drops of the suspension were placed on aluminum foil and dried at room temperature. HR-TEM samples were prepared by placing a TEM grid into a suspension of MWCNTs. Thermogravimetric analysis (TGA, STA409PC, Netzsch, Germany) was performed by heating a thermobalance from room temperature to 700 °C at a rate of 10 °C/min under a continuous nitrogen flow. Approximately, 17 mg of sample was used for analysis.

## Results and conclusion

### FTIR analysis

The FTIR spectra for p-MWCNTs, p-MWCNTs-COOH, m-MWCNTs, m-MWCNTs-1, and m-MWCNTs-2 are shown in Fig. 2. Four characteristic peaks appeared at the wavenumbers of 3432.5, 2859.0, 1739.7, and 1631.9  $\text{cm}^{-1}$ , which are assigned to –OH, –C–H, –COO, and –C=C– stretching vibrations, respectively. The peak at wavenumbers of 3432.5  $\text{cm}^{-1}$  is attributed to the stretching vibration of hydroxyl groups due to hydroxyl groups on nanotubes or the absorbed moisture attached to the nanotubes. Weak peaks at 2859.0  $\text{cm}^{-1}$  can be ascribed to asymmetric –CH<sub>2</sub> stretching. The peaks detected at 1382.7 and 1044.6  $\text{cm}^{-1}$

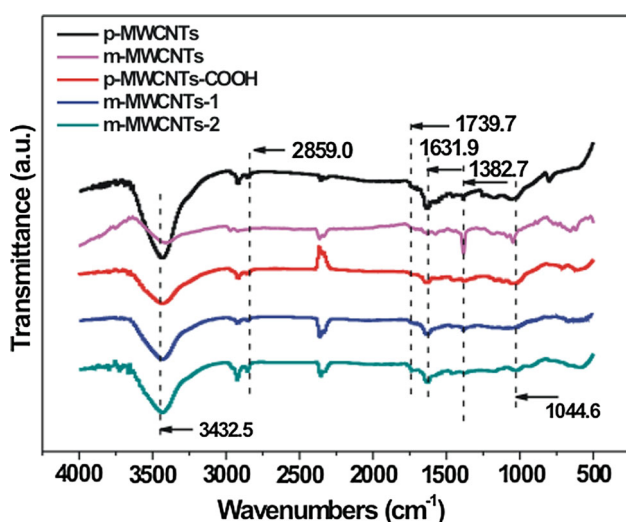


**Fig. 2** FTIR spectra of p-MWCNTs, m-MWCNTs, p-MWCNTs-COOH, m-MWCNTs-1, and m-MWCNTs-2

are assigned to bending vibration of –OH and stretching vibration of C–OH. More weak peaks appeared at 1739.7  $\text{cm}^{-1}$  are ascribed to the C=O stretching vibration of the carboxylic acid groups [22] and found in all of these samples. The intensity of this peak in the m-MWCNTs-2 is slightly higher than that in the pristine MWCNTs-COOH and m-MWCNTs-1, which confirms higher content of carboxyl groups grafted on the MWCNTs and the vital effect of ultrasonication on the oxidation process.

### Raman analysis

The functionalization of MWCNTs was further characterized by Raman analysis. Raman spectra of p-MWCNTs, m-MWCNTs, m-MWCNTs-1, and m-MWCNTs-2 in the 500–3000  $\text{cm}^{-1}$  region with a laser wavelength at 532 nm are displayed in Fig. 3. Three characteristic peaks of the D band (disorder band of sp<sup>3</sup>-hybridized carbon atoms in the nanotubes), the G band (graphite band of sp<sup>2</sup>-hybridized carbon atoms), and the G' band (second overtone of the defect induced D band) appeared at 1343.6, 1580.9, and 2680.4  $\text{cm}^{-1}$ , respectively. The relative intensity ratio of the D band to the G band,  $I_D/I_G$ , represents the degree of disorder in multi-walled carbon nanotube structures. A higher  $I_D/I_G$  implies an increase/decrease of sp<sup>3</sup>-hybridized/sp<sup>2</sup>-hybridized carbon atoms, thus implying a higher extent of functionalization of MWCNTs [9]. It can be deduced that the oxygen-containing functional groups can be grafted on the side of MWCNT according to the blue-shifted of G band (G' band) from the pristine MWCNTs 1577 (2679) to 1582 (2682), 1586 (2685)  $\text{cm}^{-1}$  for the m-MWCNTs-1 and m-MWCNTs-2, respectively [23]. However, the blue-shifted of G band (G' band) from

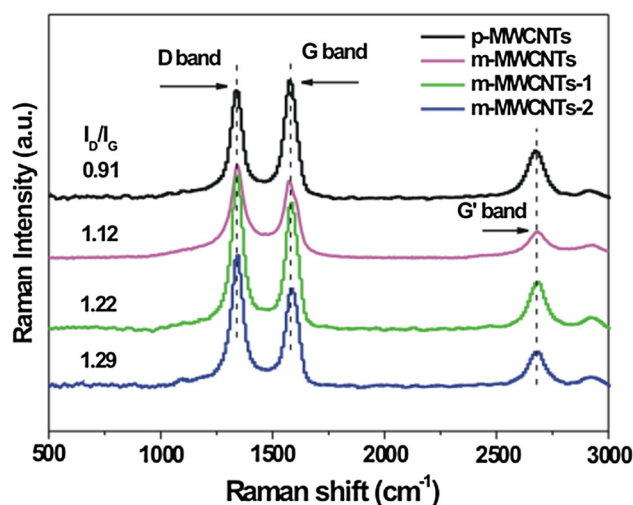


**Fig. 3** Raman spectra of p-MWCNTs, m-MWCNTs, m-MWCNTs-1, and m-MWCNTs-2 with a laser wavelength at 532 nm. The correspondent  $I_D/I_G$  is shown within the figure

the pristine MWCNTs to m-MWCNTs shows less difference, proving the weaker oxidation effect.

As expected, the relative intensity ratios  $I_D/I_G$  of m-MWCNTs ( $I_D/I_G$ : 1.12), m-MWCNTs-1 ( $I_D/I_G$ : 1.22), and m-MWCNTs-2 ( $I_D/I_G$ : 1.29) are higher than that of p-MWCNTs ( $I_D/I_G$ : 0.91). This indicates an increase of both disorder structures and the amount of the functional groups after the oxidation process. A slight difference between the m-MWCNTs-1 and m-MWCNTs-2 suggests that the higher  $I_D/I_G$  of the m-MWCNTs-2 can be attributed to the ultrasound treatment in the oxidation process. Generally, CNT structure can be destroyed by physical stress such as ultrasound treatment [23]. During the sonication process, the shockwaves and jet damage from the bubble collapse and their intense pressure and temperature improve the dispersion, leading to a high yield of oxygen-containing functional groups [8].

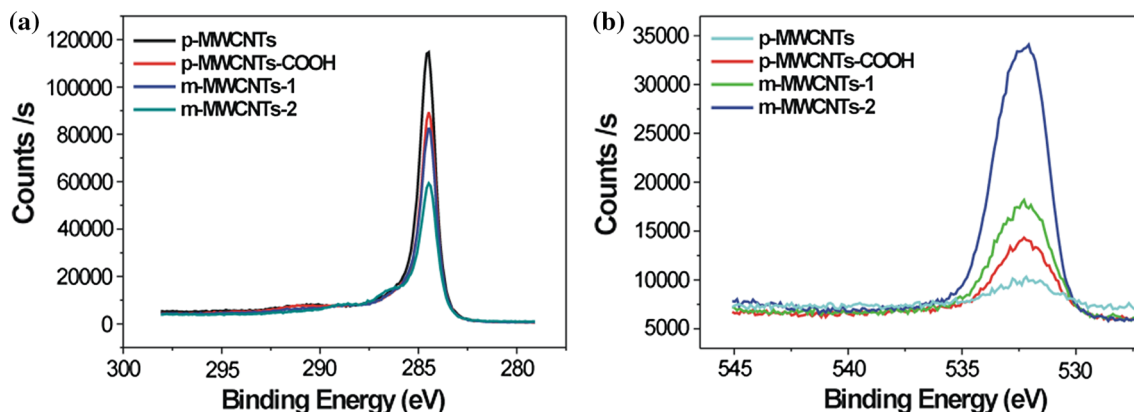
### XPS analysis

XPS spectra were used to quantify the surface elemental composition of all the MWCNTs, shown in Fig. 4. The main peaks observed for pristine and modified MWCNTs have a similar binding energy. The binding energies of the C1s and O1s are 284.09 and 531.8 eV. With XPS analysis, the increase in oxygen content is clearly observed by comparing changes in the intensity of the O1s spectra for the four different MWCNTs. The C1s peak intensity of two modified MWCNTs is much lower than that of p-MWCNTs and p-MWCNTs-COOH (Fig. 4a), whereas the O1s peak intensity of the two modified MWCNTs is much higher than that of the two commercial products (Fig. 4b).

The highest level of oxidation is found for m-MWCNTs-2. The detailed information of corresponding

element analysis and the content of O/C for all of the MWCNTs are shown in Table 1. The elements K, Na, and Mn, among others are not detected from the elements analysis, indicating that the oxidants and reagents used in the oxidation process have been completely removed. The lowest content of oxygen (2.75 at.%) is found in p-MWCNTs, which is probably attributed to the residual metal oxide present during the preparation of MWCNTs [14]. The ultrasound-assisted oxidation process typically resulted in the highest levels of oxygen (20.98 at.%). In contrast, the oxidation process without ultrasound resulted in lower levels of oxidation (9.63 at.%). After oxidation treatment of MWCNTs, the O/C ratios of m-MWCNTs-1 and m-MWCNTs-2 increase by a factor of 3 and 10, respectively.

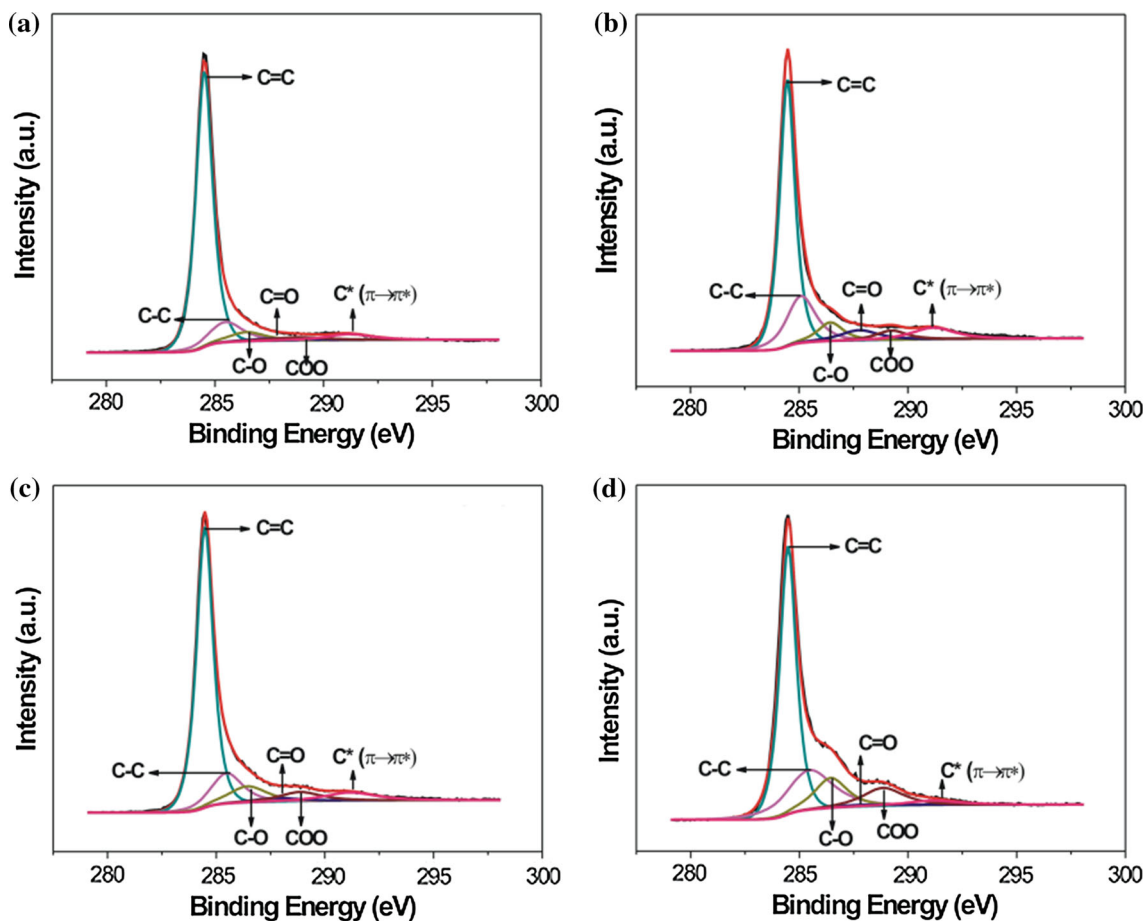
The spectra of the C1s peak for all of the MWCNTs are deconvoluted, and the contents of the different functional groups are presented in Fig. 5 and Table 2. The spectra clearly show a series of considerable changes in different functional groups, indicating that the surfaces of the MWCNTs undergo significant changes after the oxidation process. Clearly, the carboxyl contents of both of the modified MWCNTs (Fig. 5c, d) are higher than that of p-MWCNTs (2.21 at.%) and p-MWCNTs-COOH (3.87 at.%) (Fig. 5a, b). The highest carboxyl/hydroxyl content of 8.82/11.88 at.% is found for m-MWCNTs-2 with a total oxidation time of 3 h and 20 min. To our knowledge, such a high carboxyl/hydroxyl content obtained through an ultrasound-assisted oxidation process within such a short time has not been reported. This can be explained by the type and content of oxygen-containing functional groups that are sensitive to the identity of the oxidant [11]. MWCNTs treated with mild oxidants, such as  $H_2O_2$ , led to higher carboxyl/hydroxyl contents of 8.05/28.64, respectively, with an oxidation time of 6 days without ultrasonication [24].



**Fig. 4** XPS spectra corresponding to the carbon (C1s) (a) and oxygen (O1s) (b) of four different MWCNTs

**Table 1** Element content of different MWCNTs analyzed by XPS

Samples	Element contents (at.%)						
	K2p	Na1s	Mn2p	Ca2p	O1s	C1s	O/C
p-MWCNTs	N.A.			0.91	2.65	96.3	2.75
p-MWCNTs-COOH	N.A.			0.75	6.45	90.39	7.14
m-MWCNTs-1	N.A.			0.5	9.63	87.61	10.99
m-MWCNTs-2	N.A.			N.A.	20.98	72.54	28.92

**Fig. 5** XPS spectra corresponding to the carbon (C1s) of p-MWCNTs (a), p-MWCNTs-COOH (b), m-MWCNTs-1 (c), and m-MWCNTs-2 (d) are deconvoluted and the different functional groups are indicated**Table 2** The content of functional groups in different MWCNTs after deconvolution analysis

Samples (at.%)	XPS binding energy (eV)					
	284.5 C(sp <sup>2</sup> )	285.6 C(sp <sup>3</sup> )	286.4-OH	287.6-C=O	288.9-COOH	291.16 π-π*
p-MWCNTs	75.22	10.01	4.93	3.24	2.21	4.39
p-MWCNTs-COOH	58.03	19.29	6.65	5.34	3.87	6.82
m-MWCNTs-1	65.12	13.31	8.53	2.21	5.34	5.49
m-MWCNTs-2	53.57	22.17	11.88	0.96	8.82	2.61

### Thermogravimetric analysis (TGA)

The TGA results provide a quantitative evaluation of the degree of surface functionalization [9]. The effects of the types and the amounts of attached functional groups on degradation behavior and thermal stability of the MWCNTs were determined by TGA under a continuous nitrogen flow. The TGA curves and the corresponding weight loss of the carboxyl and hydroxyl groups of four different MWCNTs with a defined sample weight of 17 mg are displayed in Fig. 6. Figure 6a reveals that p-MWCNTs and p-MWCNTs-COOH remain stable at temperatures of up to 700 °C, and the total weight losses are approximately 1.8 and 5.0 wt%, respectively.

The plots of two commercial MWCNTs show a plateau at temperatures below 146 °C, which can be due to the evaporation of the adsorbed moieties on the MWCNT surfaces. The highest weight loss (approximately 2.1 wt%) of m-MWCNTs-2 may result from the presence of hydrogen bonds between water molecules and a large amount of hydroxyl groups. Then, significant weight loss appears in the temperature range from 146 to 345 °C. m-MWCNTs-1 and m-MWCNTs-2 show a weight loss of 4.1 and 6.4 wt%, respectively. The differences in weight loss can be attributed to the decarboxylation of the carboxyl groups attached on the surfaces of the multifunctional MWCNTs [25], which creates a hole in the graphene sheet, inducing the collapse of the nanotubes. The elimination of a higher content of oxygen-containing functional groups assists the structural collapse and accelerates the combustion of the nanotubes [14]. The results further support the chemical functionalization of the multifunctional MWCNTs. At temperatures between 345 and 500 °C, the weight loss of the m-MWCNTs-1 and m-MWCNTs-2 is approximately 2.6 and 4.1 wt%, respectively. The thermal degradation in this temperature range

may originate from the elimination of the hydroxyl functionalities [25]. The weight loss at temperatures above 500 °C is mainly caused by the removal of the remaining amorphous carbons. Compared with other mild oxidation process with ultrasonication, the weight loss is less than 2 % at 500 °C, while about 13 % weight in Fig. 6a. These indicate the content of the oxygen-containing functional groups by our approach is higher than others.

The results of four different MWCNTs from TGA and XPS are compared in Fig. 6b. All of the MWCNTs on the X-axis were arranged according to the amount of functional groups. The weight loss of the functional groups from TGA is reasonably well correlated with the amount of functional groups in different MWCNTs from XPS. The weight loss increases with the amount of functional groups, for either carboxyl groups or hydroxyl groups. Because the two modified MWCNTs contain much higher contents of functional groups than the commercial MWCNTs, higher weight loss for individual functional groups was determined. Especially for m-MWCNTs-2, the maximum values of weight loss for both carboxyl and hydroxyl groups were found. The TGA analysis of these samples clearly indicates that relatively high amounts of carboxyl and hydroxyl groups existed on MWCNT surfaces for both of the modified MWCNTs. As shown, the results from the TGA were consistent with those obtained from XPS, demonstrating that TGA can be an alternative method to provide more quantitative identification of surface functional groups in addition to acid titration, pH measurement, and energy-dispersive X-ray spectroscopy EDX [11].

### Dispersion observation by photography and particle size analyzer

The presence of functional groups on the MWCNTs was further identified by observing the dispersion of MWCNTs

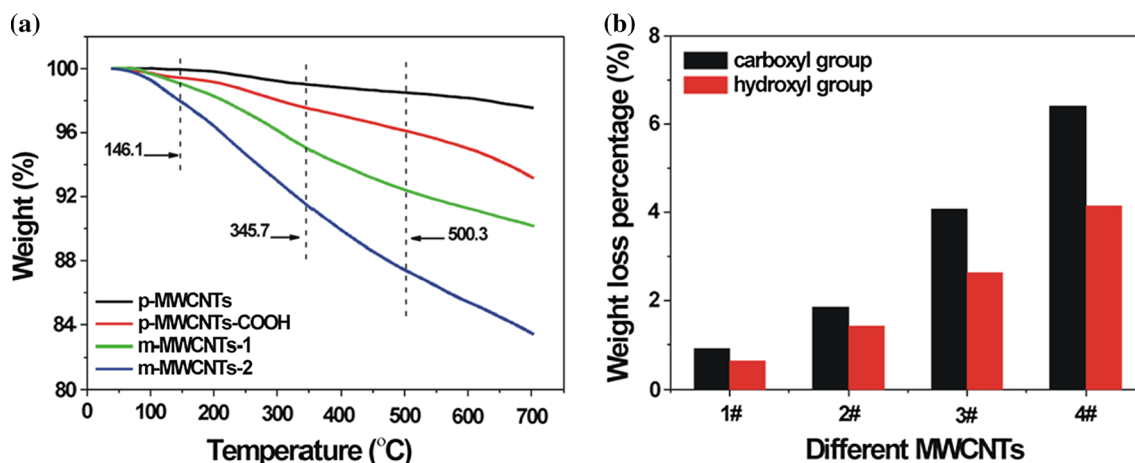


**Fig. 6** TGA curves (a), weight loss of carboxyl groups and hydroxyl groups (b) of p-MWCNTs (1#), p-MWCNTs-COOH (2#), m-MWCNTs-1 (3#), and m-MWCNTs-2 (4#) are displayed

in ethanol with photography, and the effect of oxidation on the particle size of MWCNTs in water was determined by a laser particle size analyzer. The dispersibility of MWCNTs in ethanol was determined by mixing 0.02 g MWCNTs in 20 ml ethanol, followed by sonication for 10 min. The dispersion stability of MWCNT mixtures with time points of 1 h, 10 h, 3.5, and 7 days was photographed and is shown in Fig. 7. Two commercially available MWCNTs, p-MWCNTs, p-MWCNTs-COOH, were selected for a comparison to understand the effect of the functional group on the dispersibility.

Because pristine MWCNTs have a strong tendency to entangle and aggregate due to their high surface energy, the sedimentation of p-MWCNTs in ethanol occurred 1 h after preparation, as shown in Fig. 7a. The p-MWCNTs-COOH partially separated from ethanol 7 d after preparation (Fig. 7b). Surprisingly, no significant change was observed from the dispersion state of the m-MWCNTs-1 (Fig. 7c) and m-MWCNTs-2 (Fig. 7d) in ethanol after 7 days. After 30 days, the m-MWCNTs-1 began to separate from the

ethanol; however, m-MWCNTs-2 remained in the dispersion state. This again confirms that higher carboxyl and hydroxyl content is present in m-MWCNTs-2. The introduction of a higher content of carboxyl and hydroxyl groups (Table 2) through this oxidation process resulted in more negative charges, which resulted in the long-term electrostatic stability required for the dispersion of the CNTs in liquid medium [9]. Therefore, the dispersibility of the modified MWCNTs in ethanol was remarkably improved.

For a better understanding of the effect of the agglomerate size on the dispersibility of different MWCNTs in solvent, a particle size distribution of MWCNTs in water was analyzed using a laser size distribution analyzer. Figure 8a shows that the p-MWCNTs have a broad particle size distribution centered at approximately 50  $\mu\text{m}$ . The percentage of the agglomerates with sizes below 70  $\mu\text{m}$  is approximately 83 %, whereas the p-MWCNTs-COOH possess a bimodal distribution with two peaks centered at 10 and 27  $\mu\text{m}$ . The percentage of the agglomerates with sizes below 15  $\mu\text{m}$  is approximately 81 % Fig. 8b.

The length of two CNTs provided by the company is within the range of 10–30  $\mu\text{m}$ . Apparently, strong aggregation is found for the pristine MWCNTs, which is in good agreement with the literature [26]. However, the p-MWCNTs-COOH disperse uniformly in aqueous solution and show little aggregation due to their deionization; therefore, they have a better dispersion than the p-MWCNTs [27]. This is attributed to the addition of oxygen-containing functional groups, which destroyed the integrity of the MWCNT structure and lowered the van der Waals force among the MWCNTs [9]. A similar size distribution was found for the m-MWCNTs-1 in Fig. 8c because the carboxyl contents in both of the carboxylated MWCNTs are similar (Table 2). For the m-MWCNTs-2 (Fig. 8d), a monodisperse distribution curve centered at approximately 8  $\mu\text{m}$  is observed, and the percentage of particle sizes below 12  $\mu\text{m}$  accounts for 98 %. The decrease in particle size results in a decrease of aggregation, resulting in a better dispersion of the m-MWCNTs-2 in water. Note that the size is referred to the size of MWCNT agglomerations rather than the length or diameter of the multi-walled nanotubes.

### Morphology observation by FESEM and HR-TEM

The purpose of functionalizing the MWCNTs was to obtain a better dispersibility in solvent without shortening or severely damaging their structures. To observe the dispersion stability and surface morphology of the nanotubes, an FESEM analysis of four different MWCNTs was performed and is shown in Fig. 9.

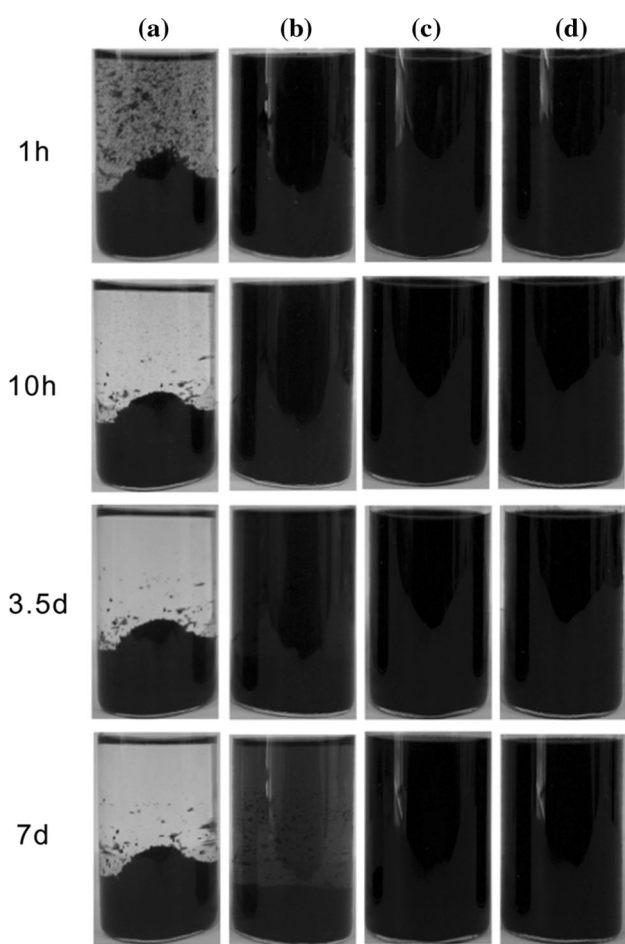


**Fig. 7** Photographs of four MWCNTs dispersed in ethanol for 1 h, 10 h, 3.5, and 7 days. **a** p-MWCNTs; **b** p-MWCNTs-COOH; **c** m-MWCNTs-1; and **d** m-MWCNTs-2



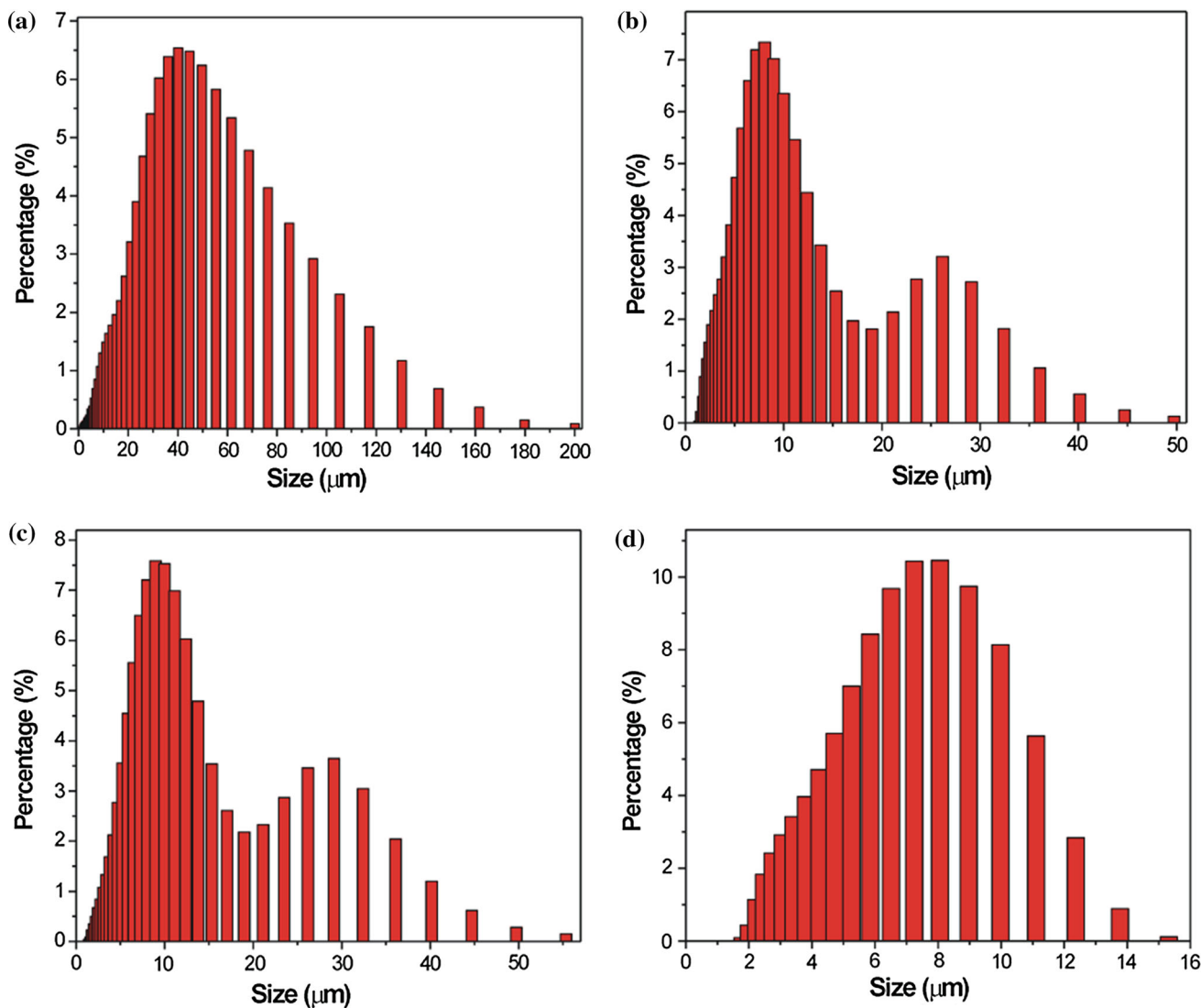


**Fig. 8** Particle size distribution of four different MWCNTs in water. **a** p-MWCNTs; **b** p-MWCNTs-COOH; **c** m-MWCNTs-1; and **d** m-MWCNTs-2

Obviously, the p-MWCNTs entangle together and form a bundle of tubes due to their high aspect ratio and van der Waals forces (Fig. 9a). The functionalized MWCNTs become less entangled and show no apparent damage on the sidewalls of MWCNTs (Fig. 9b–d). This can be ascribed to the presence of the carboxyl content, which reduces their surface energy. As illustrated by the red arrow in Fig. 9c, the m-MWCNTs-1 surface contains some agglomerates and is poorly dispersed in the solvent compared with the m-MWCNTs-2.

To assess the effect of the oxidation process on the MWCNT diameters, the content of defect sites in the MWCNT sidewalls, and the dispersibility of the MWCNTs in solvent, an HR-TEM analysis of the pristine MWCNTs and the functionalized MWCNTs was performed and is

shown in Fig. 10. Clearly, the p-MWCNTs contain fewer defect sites and have little amorphous carbon tangled around the sidewalls, which are smooth and uniform. For the p-MWCNTs-COOH and the m-MWCNTs-1, a few defect sites are generated on their sidewall surfaces, and their diameters become smaller. On the contrary, HR-TEM images of m-MWCNTs-2 show different surface morphologies in comparison to p-MWCNTs, p-MWCNTs-COOH, and m-MWCNTs-1 (Fig. 10a–c). Although the m-MWCNTs-2 (Fig. 10d) was exposed to three different oxidants, the coarse sidewalls with uniformly distributed defect sites imply that the oxygen-containing groups are successfully introduced on the sidewalls of the m-MWCNTs-2. The less-damaged functionalized CNT prepared by the ultrasound-assisted oxidation method in

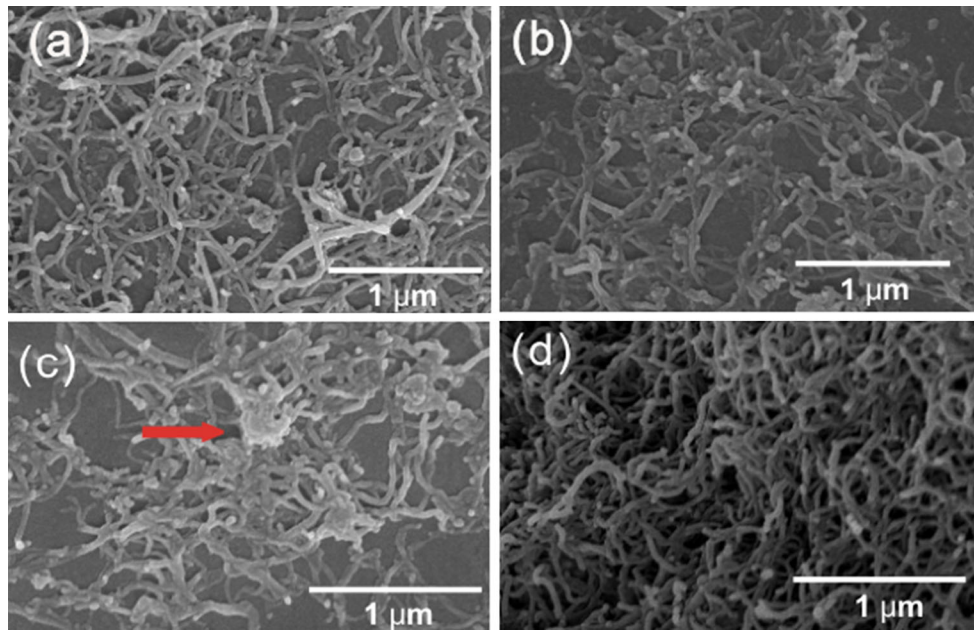


**Fig. 9** Surface morphologies of four different MWCNTs. **a** p-MWCNTs; **b** p-MWCNTs-COOH; **c** m-MWCNTs-1; and **d** m-MWCNTs-2

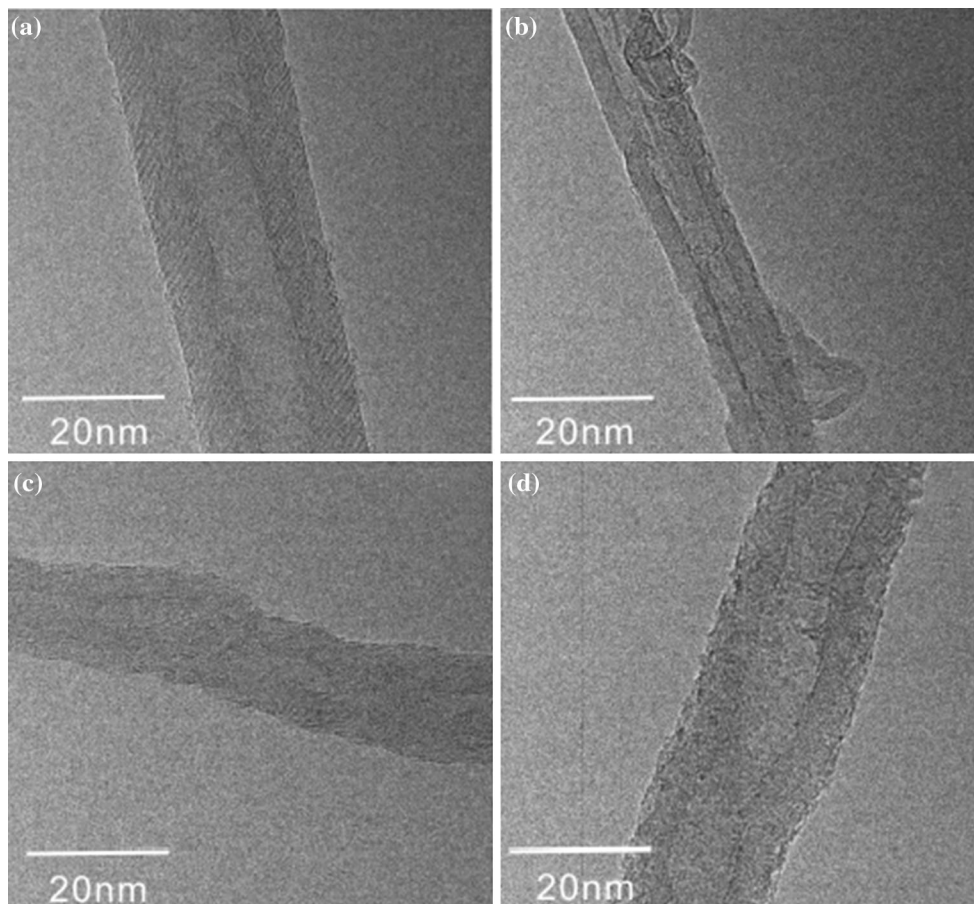


**Fig. 10** TEM analysis of four different MWCNTs. **a** p-MWCNTs; **b** p-MWCNTs-COOH; **c** m-MWCNTs-1; and **d** m-MWCNTs-2

this study can be due to mild acid oxidation treatment with low power sonication, which has been confirmed in the other study [20].

## Conclusion

Multifunctionalized MWCNTs have a high reactivity with many chemicals and a better dispersibility in liquid media; in addition, they incorporate flexibility in polymer composites. In this study, carboxyl and hydroxyl groups on the surface of the MWCNTs were successfully introduced to obtain multifunctionalization of MWCNTs by the three-component oxidant treatment with the aid of ultrasonication. The mild three-stage-oxidation method appears to be efficient with no apparent structural damage to the tubes and creates functionalized MWCNTs with an ultrahigh fraction of both carboxyl and hydroxyl groups within a shorter reaction time. FTIR, Raman, and XPS results verify the presence of carboxyl, carbonyl, and hydroxyl groups on the functionalized MWCNTs. The ultrasonicated MWCNTs exhibit advantages over the non-ultrasonicated MWCNTs in the form of a significantly higher carboxyl content, better dispersibility in solvents, and a smaller size of agglomerates. FESEM and HR-TEM show better dispersion and less damage on the sidewalls of the modified MWCNTs. A TGA analysis further proves the existence of different functional groups by evaluating the weight loss over different temperature ranges. A quantitative correlation between TGA and XPS is first reported, which demonstrates that TGA can potentially be used to provide a more quantitative identification of surface functional groups.

**Acknowledgement** The authors gratefully acknowledge financial support from the National Natural Science Foundation of China (11344007), and the Natural Science Foundation of Tianjin, China (12JCZDJC27300).

## Compliance with ethical standards

**Conflict of Interest** The authors declare that they have no conflict of interest.

## References

- Lalwani G, Henslee AM, Farshid B, Lin L, Kasper FK, Qin Y-X et al (2013) Two-dimensional nanostructure-reinforced biodegradable polymeric nanocomposites for bone tissue engineering. *Biomacromolecules* 14:900–909
- Daraei P, Madaeni SS, Ghaemi N, AliKhadivi M, Astinchap B, Moradian R (2013) Enhancing antifouling capability of PES membrane via mixing with various types of polymer modified multi-walled carbon nanotube. *J Membr Sci* 444:184–191
- Chang TE, Kisliuk A, Rhodes SM, Brittain WJ, Sokolov AP (2006) Conductivity and mechanical properties of well-dispersed single-wall carbon nanotube/polystyrene composite. *Polymer* 47:7740–7746
- Amr IT, Al-Amer A, Al-Harhi M, Gire SA, Sougrat R et al (2011) Effect of acid treated carbon nanotubes on mechanical, rheological and thermal properties of polystyrene nanocomposites. *Compos Part B* 42:1554–1561
- Kim JA, Seong DG, Kang TJ, Youn JR (2006) Effects of surface modification on rheological and mechanical properties of CNT/epoxy composites. *Carbon* 44:1898–1905
- Geng Y, Liu MY, Li J, Shi XM, Kim JK (2008) Effects of surfactant treatment on mechanical and electrical properties of CNT/epoxy nanocomposites. *Compos Part A* 39:1876–1883
- Damian CM, Garea SA, Vasile E, Iovu H (2012) Covalent and non-covalent functionalized MWCNTs for improved thermo-mechanical properties of epoxy composites. *Compos Part B* 43:3507–3515
- Ng CM, Manickam S (2013) Improved functionalization and recovery of carboxylated carbon nanotubes using the acoustic cavitation approach. *Chem Phys Lett* 557:97–101
- Zhao Z, Yang Z, Hu Y, Li J, Fan X (2013) Multiple functionalization of multi-walled carbon nanotubes with carboxyl and amino groups. *Appl Surf Sci* 276:476–481
- Dominguez DD, Laskoski M, Keller TM (2009) Modification of oligomeric cyanate ester polymer properties with multi-walled carbon nanotube-containing particles. *Macromol Chem Phys* 210:1709–1716
- Wepasnick KA, Smith BA, Schrote KE, Wilson HK, Diegelmann SR, Fairbrother DH (2011) Surface and structural characterization of multi-walled carbon nanotubes following different oxidative treatments. *Carbon* 49:24–36
- Dimiev AM, Tour JM (2014) Mechanism of graphene oxide formation. *ACS Nano* 8:3060–3068
- Cruz-Silva R, Morelos-Gomez A, Vega-Diaz S, Tristan-Lopez F, Elias AL, Perea-Lopez N et al (2013) Formation of nitrogen-doped graphene nanoribbons via chemical unzipping. *ACS Nano* 7:2192–2204
- Martín O, Gutierrez HR, Maroto-Valiente A, Terrones M, Blanco T, Baselga J (2013) An efficient method for the carboxylation of few-wall carbon nanotubes with little damage to their sidewalls. *Mater Chem Phys* 140:499–507
- Zschoerper NP, Katzenmaier V, Vohrer U, Haupt M, Oehr C, Hirth T (2009) Analytical investigation of the composition of plasma-induced functional groups on carbon nanotube sheets. *Carbon* 47:2174–2185
- Mallakpour S, Zadehnazari A (2014) A facile, efficient, and rapid covalent functionalization of multi-walled carbon nanotubes with natural amino acids under microwave irradiation. *Prog Org Coat* 77:679–684
- Saito T, Matsushige K, Tanaka K (2002) Chemical treatment and modification of multi-walled carbon nanotubes. *Phys B* 323:280–283
- Saleh NB, Pfefferle LD, Elimelech M (2008) Aggregation kinetics of multiwalled carbon nanotubes in aquatic systems: measurements and environmental implications. *Environ Sci Technol* 42:7963–7969
- Hennrich F, Krupke R, Arnold K, Stutz JAR, Lebedkin S, Koch T (2007) The Mechanism of cavitation-induced scission of single-walled carbon nanotubes. *J Phys Chem B* 111:1932–1937
- Aviles F, Cauich-Rodriguez JV, Moo-Tah L, May-Pat A, Vargas-Coronado R (2009) Evaluation of mild acid oxidation treatments for MWCNT functionalization. *Carbon* 47:2970–2975
- Yang D-Q, Rochette J-F, Sacher E (2005) Functionalization of multiwalled carbon nanotubes by mild aqueous sonication. *J Phys Chem B* 109:7788–7794

22. Hsua H-L, Jehng J-M, Sung Y, Wang L-C, Yang S-R (2008) The synthesis, characterization of oxidized multi-walled carbon nanotubes, and application to surface acoustic wave quartz crystal gas sensor. *Mater Chem Phys* 109:148–155
23. Torres D, Pinilla JL, Moliner R, Suelves I (2015) On the oxidation degree of few-layer graphene oxide sheets obtained from chemically oxidized multiwall carbon nanotubes. *Carbon* 81:405–417
24. Peng Y, Liu H (2006) Effects of oxidation by hydrogen peroxide on the structures of multiwalled carbon nanotubes. *Ind Eng Chem Res* 45:6483–6488
25. Datsyuk V, Kalyva M, Papagelis K, Parthenios J, Tasis D, Siokou A (2008) Chemical oxidation of multiwalled carbon nanotubes. *Carbon* 46:833–840
26. Kim SW, Kim T, Kim YS, Choi HS, Lim HJ, Yang SJ (2012) Surface modifications for the effective dispersion of carbon nanotubes in solvents and polymers. *Carbon* 50:3–33
27. Liebscher M, Gärtner T, Tzounis L, Micušíkc M, Pötschke P, Stamm M (2014) Influence of the MWCNT surface functionalization on the thermoelectric properties of melt-mixed polycarbonate composites. *Compos Sci Technol* 101:133–138